Optical Fibers for Flexible Networks and Systems [Invited]

John D. Downie, Ming-Jun Li, and Sergejs Makovejs

***Abstract*—The attributes and characteristics of optical transmission fibers have evolved over the years to accommodate different system technologies and optimize overall system performance. In the emerging era of elastic or flexible networks, optical fibers will continue to play a key role in determining system reach and capacity. In this paper, we examine key characteristics of optical fibers for coherent transmission systems and review recent results that highlight the performance differences observed between fiber designs and between data rates such as 100 and 200 Gbits/s per channel that describe transceivers in current and near-future flexible networks.**

***Index Terms*—Fiber optics communications; Optical fibers.**

I. Introduction

Since the first demonstration of optical fiber with attenuation less than 20 dB/km in 1970 [1], optical fibers and transmission systems have evolved simultaneously in the steady and spectacular progress of optical communications. Together, advances in fiber, component, and system technologies have enabled the transmission capacity of a single fiber to increase on average by a factor of approximately 10 every four years from the beginning of the industry to the present time [2].

Long-haul transmission systems in particular have changed significantly over the years, described by several clear generations. The first optical fiber communication systems were comprised of LED sources emitting in the 850 nm wavelength region and transmitted over multimode optical fibers (MMFs) [3]. However, MMFs have fundamental bandwidth limitations because of intermodal dispersion, and these early systems quickly gave way to systems employing single-mode optical fiber with the advent of single-mode semiconductor lasers in the late 1970s [4]. These single-mode fiber systems were initially built and deployed to operate in the 1310 nm wavelength range, largely because the zero-chromatic-dispersion wavelength of a standard step-index single-mode fiber occurs in that region [5–7].

However, the lowest attenuation region of single-mode fiber lies in the 1550 nm wavelength window, and this fact prompted the next move in transmission systems and fiber technologies to that part of the spectrum. While attenuation is lowest around 1550 nm, chromatic dispersion is relatively large at approximately 17 ps/nm/km for standard single-mode fiber. To keep the barrier of dispersion from inhibiting growth in data rates at 1550 nm, dispersion-shifted optical fibers (DSFs) were first developed that moved the zero-dispersion wavelength also to 1550 nm [8–11]. While this worked well for single-channel systems operating at 1550 nm, the advent of erbium-doped fiber amplifiers (EDFAs) ushered in the age of wavelength-division-multiplexed (WDM) systems, and it was soon discovered that impairments from the nonlinear effect of four-wave mixing could severely degrade the performance of multiple-wavelength systems [12]. Furthermore, this effect is exacerbated by WDM transmission in DSF with the zero-dispersion wavelength in the transmission wavelength band, thus enhancing the nonlinear effect [13]. This knowledge then provided the motivation to further change fiber designs to ensure at least a nominal level of positive dispersion in the 1550 nm window in an effort to balance the impairments from dispersion and four-wave mixing, leading to nonzero-dispersion-shifted fibers (NZ-DSFs) that had typical dispersion values of 3–8 ps/nm/km at 1550 nm [14–17]. Further innovation in NZ-DSFs then reduced nonlinear impairments again using designs that increased the effective area from typical values around 50 μm^2 to about 72 μm^2, improving 2.5 and 10 Gbit/s WDM transmission performance and leading to widespread deployment [18–21].

Most recently, long-haul and ultra-long-haul optical transmission systems have undergone another significant change with the technologies of advanced multilevel modulation formats and coherent detection [22,23]. With coherent receivers and advanced digital signal processing (DSP) in both transmitters and receivers, modulation formats encoded in both amplitude and phase are possible with varying levels of complexity, to produce signals with different data rates. Examples of formats include binary phase-shift keying (BPSK), quadrature phase-shift keying (QPSK), 8 quadrature amplitude modulation (8QAM), and 16QAM, as well as many other potential formats that can now be realized. Coherent receivers also enable independent data to be encoded on two orthogonal polarizations. For the same symbol rate, different formats such as those listed above each have different requirements in terms of optical signal-to-noise ratio (OSNR) to meet the same bit error rate (BER). In principle, flexible transceivers

Manuscript received January 7, 2016; revised March 18, 2016; accepted March 29, 2016; published April 22, 2016 (Doc. ID 257059).

The authors are with Corning Incorporated, One Riverfront Plaza, Corning, New York 14831, USA (e-mail: downiejd@corning.com).

http://dx.doi.org/10.1364/JOCN.8.0000A1

can then switch between formats using the same hardware to produce signals that maximize the data rate on an optical channel for a given link OSNR budget. This is indeed a key idea behind flexible or elastic networks.

For fiber plant, one of the main consequences of coherent transmission systems is that all chromatic dispersion compensation can now be performed digitally in the receiver, or divided between the transmitter and receiver. Similarly, polarization mode dispersion (PMD) can also be compensated in the digital coherent receiver. Thus new systems are built without any optical dispersion compensation in-line, as was previously characteristic of dispersion-managed systems. Not only is it simpler and more cost-effective to compensate dispersion digitally, but the nonlinear performance of coherent systems is significantly improved without in-line optical dispersion management [23,24]. For optical fiber, the most important characteristics now boil down rather simply to attenuation and nonlinear tolerance, as these are the characteristics that directly affect OSNR. However, these fiber parameters are very important, as they can largely determine the optical reach of the various formats available to be transmitted and received in emerging elastic networks. In this paper, we examine the performance levels possible with different fiber designs and potential reach lengths under different system and amplification schemes.

II. Optical Fibers for Coherent Systems

A. Long-Haul Repeatered Systems

As mentioned above, the key fiber parameters affecting system performance for new coherent systems are attenuation and nonlinear tolerance. A fiber figure of merit (FOM) has been developed based on the Gaussian noise model of coherent transmission systems to evaluate the expected performance of different fibers [25]. We use a simplified version of that fiber FOM, as given in Eq. (1) below, in which the FOM is defined relative to a reference fiber, and it is assumed that dispersion is essentially equivalent for high-dispersion fibers such as those described by the International Telecommunication Union Telecommunication Standardization Sector G.654 standard [26]. The amplifier noise figure is assumed to be constant for all fibers, miscellaneous loss components are ignored, and optimal launch power into each span is assumed for all fibers:

$$\mathrm{FOM(dB)} = \frac{2}{3}\left(10\log\left[\frac{A_{\mathrm{eff}}\cdot n_{2,\mathrm{ref}}}{A_{\mathrm{eff,ref}}\cdot n_2}\right] - [\alpha_{\mathrm{dB}} - \alpha_{\mathrm{ref,dB}}]\cdot L\right) - \frac{1}{3}\left(10\log\left[\frac{L_{\mathrm{eff}}}{L_{\mathrm{eff,ref}}}\right]\right). \quad (1)$$

In Eq. (1), A_{eff} is the fiber effective area, n_2 is the nonlinear index of refraction, α_{dB} is the fiber attenuation in units of dB/km, L is the span length of the repeatered system being considered, and L_{eff} is the nonlinear effective length. The terms with "ref" in the subscript refer to the reference fiber. The effective length L_{eff} is defined as follows (where α is in linear units):

$$L_{\mathrm{eff}} = \frac{(1-\exp[-\alpha L])}{\alpha} \approx \frac{1}{\alpha}. \quad (2)$$

As defined here and based on the Gaussian noise model, the fiber FOM represents the expected difference in the 20 log(Q) value between the fiber under evaluation and the reference fiber in the coherent system. The FOM results of Eq. (1) are shown in Fig. 1, where the reference fiber is chosen to have an attenuation of 0.2 dB/km and A_{eff} of 80 μm^2, roughly comparable to many standard single-mode fibers. The span length represented in Fig. 1 is 100 km. The data in Fig. 1 clearly show that reducing the fiber attenuation and/or increasing the effective area leads to increased FOM and better system performance. For example, a fiber with an attenuation of 0.165 dB/km but the same A_{eff} has a performance advantage of about 2.3 dB compared to the reference fiber. If the effective area is increased to 150 μm^2 with 0.155 dB/km attenuation, the performance advantage increases to about 4.7 dB. In Fig. 1, note that there is a discontinuity between the attenuation values of 0.174 and 0.175 dB/km. This reflects the assumption made here that attenuation values below 0.175 dB/km are achieved with pure silica core fibers with a lower nonlinear index n_2 compared to Ge-doped silica core fibers [26,27]. The values of n_2 assumed in Fig. 1 are 2.3×10^{-20} m^2/W for Ge-doped fiber and 2.1×10^{-20} m^2/W for silica core fiber.

While Fig. 1 shows that better performance can be obtained by both lowering fiber attenuation and increasing the effective area, it can also be interesting to examine the relative strength of those two parameters as a function of span length [28,29]. In Fig. 2, we calculate the equivalent increase in the effective area as a function of the reduction of the fiber attenuation, as defined by having the same increase in FOM with regard to the reference fiber nominal parameters. This is done for four different span lengths of 120, 100, 80, and 60 km. Figure 2 demonstrates that lowering the fiber attenuation has a larger effect for longer spans. For example, a reduction in attenuation (from 0.2 dB/km) of −0.04 dB/km is equivalent to increasing the effective area (above 80 μm^2) by approximately 155, 120, 85, and 60 μm^2 for span lengths of 120, 100, 80, and 60 km, respectively. Alternatively, one may say that an increase in the fiber effective area is equivalent to a larger decrease in attenuation for shorter span lengths in terms of FOM.

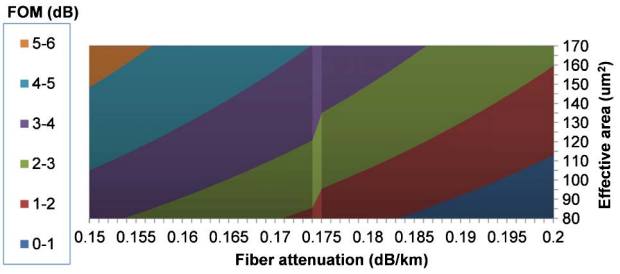

Fig. 1. Fiber FOM as a function of attenuation and effective area for 100 km spans in a long-haul repeatered system.

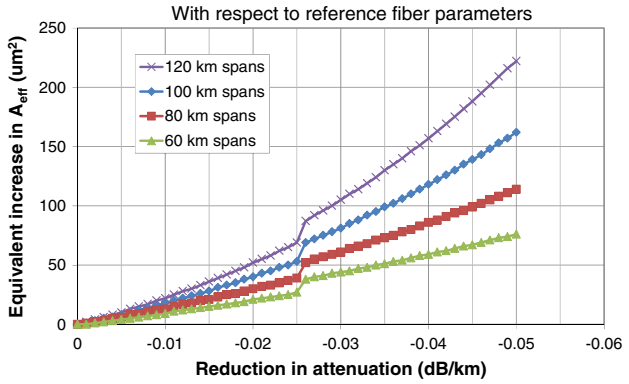

Fig. 2. Equivalent increase in effective area as a function of attenuation reduction for four different span lengths.

We now turn to experimental transmission measurements made to compare different optical fibers and signals with data rates of 100 and 200 Gbits/s to assess their relative performance, primarily in terms of optical reach. We first look at a straight comparison of four fibers in the same system configuration with EDFA amplification. The experimental setup is shown in Fig. 3 and was described for three of the fibers previously [30]. The transmission system in each case had 20 channels with dense wavelength division multiplexing (DWDM) 50 GHz channel spacing, each modulated at 256 Gbits/s with 32 Gbaud polarization-multiplexed (PM)-16QAM signals. The span length was 100 km, and the recirculating loop was comprised of three spans.

The four fibers evaluated in the experiments were G.652-compliant Corning® SMF-28e+® and Corning SMF-28® ULL fiber and two G.654-compliant fibers with larger effective areas, Corning Vascade® EX2000 and Vascade EX3000 fibers. The effective areas of the fibers and the average span losses constructed from the fibers used in the tests are provided in Table I.

Results for the Q factors of the center channel at 1550.92 nm derived from BER measurements made by direct error counting are shown in Fig. 4. For each fiber

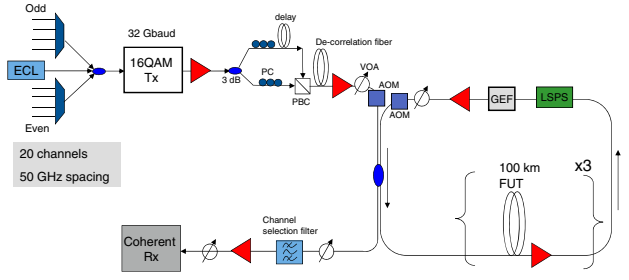

Fig. 3. Experimental setup for transmission performance measurements of four optical fibers for EDFA systems. ECL, external cavity laser; Tx, transmitter; PC, polarization controller; PBC, polarization beam combiner; VOA, variable optical attenuator; AOM, acousto-optic modulator; GEF, gain equalization filter; LSPS, loop synchronous polarization scrambler; FUT, fiber under test; Rx, receiver.

TABLE I
FIBER PARAMETERS

	SMF-28e+	SMF-28 ULL	Vascade EX2000	Vascade EX3000
Average span loss (dB)	19.2	16.7	16.3	16.1
Nominal A_{eff} (μm^2)	82	82	112	150

type, the optimal launch power per channel was first determined at a distance of 600 km before the rest of the measurements were taken at all other distances. The optimal channel powers determined were −1, 0, 0, and +1 dBm for SMF-28 ULL, SMF-28e+, Vascade EX2000, and Vascade EX3000, respectively. The assumed 20log(Q), or dBQ, threshold for error-free detection for 23% overhead soft decision forward error correction (SD-FEC) was 6.25 dB, or 2.0×10^{-3} BER. As shown in Fig. 4, the four fibers have distinctly varying performance levels depending on their characteristics.

As compared to what is predicted in Q differences at a given distance from the FOM results in Fig. 1, the actual differences are somewhat smaller due to multiple effects. Some of these effects include (1) the transmitter/receiver back-to-back performance, (2) the finite OSNR of the signals on launch into the loop, (3) the larger negative effect of the extra loop EDFA on systems with lower fiber attenuation, and (4) the somewhat higher noise figure of the laboratory EDFAs for smaller gains required by the lower attenuation fibers. The last three effects can be represented by calculating an effective noise figure (NF_{eff}) for the amplifiers after each span as a function of transmission distance. Values for the calculated NF_{eff} as well as model results are given in Fig. 5, illustrating the differences between the systems with different fibers. NF_{eff} is calculated by treating the measured OSNR as if it pertains to a simple straight-line system, and NF_{eff} is the noise figure of each EDFA. The model used calculated OSNR values according to the characteristics of the amplifiers in the experimental system. In principle, much of the differences in the effective amplifier noise figure could be eliminated in

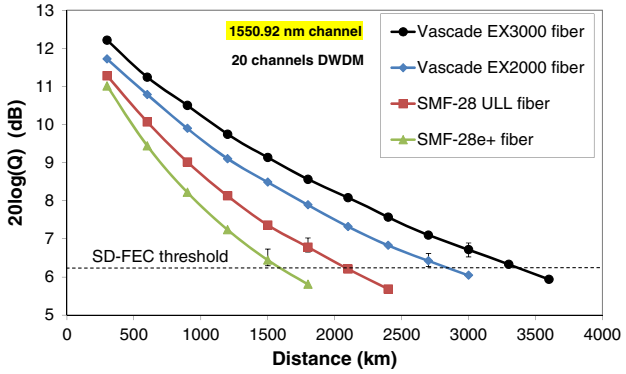

Fig. 4. Transmission performance for 256 Gbit/s PM-16QAM signals over four different optical fibers with EDFA systems.

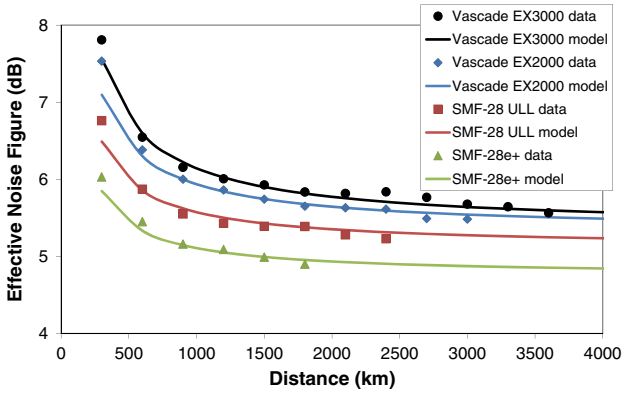

Fig. 5. Effective noise figure calculated for EDFA systems from OSNR measurement data and modeled results.

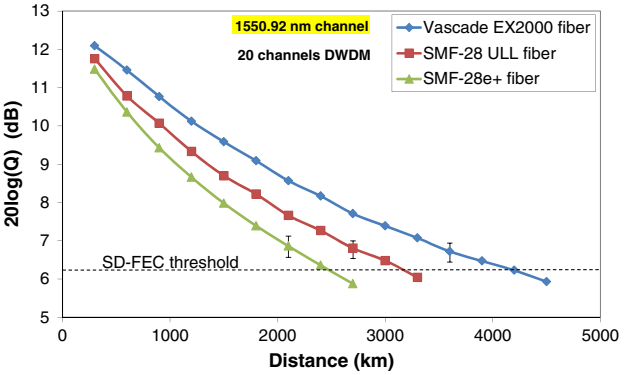

Fig. 6. Transmission performance for 256 Gbit/s PM-16QAM signals over three different optical fibers with Raman systems.

real straight-line systems, accentuating the performance advantages of the ultralow attenuation fibers.

In addition to the effects present in the laboratory recirculating loop systems described above, there were also differing chromatic dispersion values of the fibers, especially for the two G.652 fibers compared to the two G.654 fibers, that were assumed to be negligible in Eq. (1) and Fig. 1 but likely did have some effect in practice. However, overall the results clearly indicate the better performance of the fibers with lower attenuation and/or larger effective areas, both in dBQ at a given distance, and in enabling longer transmission reach as defined by the maximum transmission distance before reaching the FEC threshold. In fact, the increases in the transmission reach of the SMF-28 ULL, Vascade EX2000, and Vascade EX3000 fibers were about 32%, 80%, and 115%, respectively, compared to the standard single-mode fiber SMF-28e+.

While the previous results were obtained for transmission over EDFA systems, similar differences in performance for different fibers are observed for long-haul repeatered systems using distributed Raman amplification [30]. We investigated 256 Gbit/s PM-16QAM transmission with a similar experimental setup to that in Fig. 3, except that backward-pumped Raman amplification was used to compensate for each span loss rather than an EDFA. The three Raman pump wavelengths employed were 1427, 1443, and 1462 nm. Results for Q factor versus transmission distance using the optimal channel launch powers for the Raman systems corresponding to three optical fibers studied are shown in Fig. 6.

The general trends and relative performance of the fibers in the Raman system are comparable to those in the EDFA system, although on average the Raman amplified systems have about 50% longer reach lengths. For example, the relative ordering of optimal channel launch power of the three fibers was the same as for the EDFA systems, ranging for the Raman systems from −3.5 dBm for SMF-28 ULL fiber to −2.5 dBm for Vascade EX2000 fiber. However, we note that the effect of the extra EDFA in the loop to compensate for the loop component loss is larger for Raman systems, because the noise figure of the EDFA is significantly larger than the noise figures of the Raman amplifiers. This tends to artificially reduce the reach values that would be possible in a straight-line system with only Raman amplifiers.

As is predicted by theory, the required OSNR for PM-QPSK signals is almost 7 dB lower than for PM-16QAM signals with the same symbol rate to achieve the same BER [23]. We explored this by transmitting 112 Gbit/s PM-QPSK signals over the same Raman amplified systems as the 256 Gbit/s PM-16QAM signals. While the symbol rate for the PM-QPSK channels was 28 Gbaud instead of 32 Gbaud, these are close enough to make the comparison. For this set of experiments, we transmitted 40 channels over the same three fibers. The results in terms of Q factor for the center channel at 1550.92 nm are given in Fig. 7.

As anticipated, the reach lengths for 112 Gbit/s PM-QPSK channels are significantly longer than for 256 Gbit/s PM-16QAM channels. Note that the FEC threshold is assumed to be 8.5 dBQ here, with only 7% FEC overhead. Regardless of the FEC thresholds, the achieved distances for the 112 Gbit/s channels were about 7× longer than for the 256 Gbit/s channels for the same Q-factor value. This level of difference in reach between QPSK and 16QAM channels has been well documented by other researchers as well [31]. The required OSNR values for the same Q factor were almost 11 dB higher for the

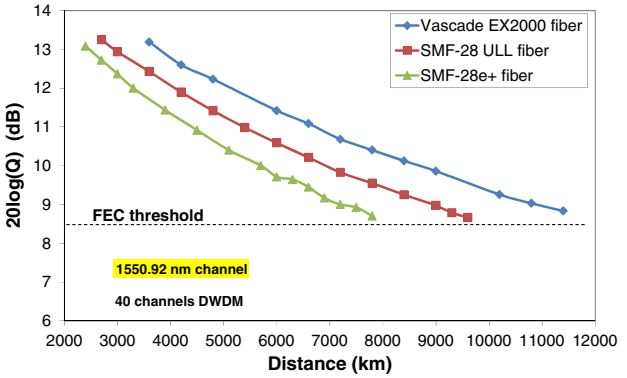

Fig. 7. Transmission performance for 112 Gbit/s PM-QPSK signals over three different optical fibers with Raman systems.

16QAM signal. This is consistent with theory, adjusting for the different symbol rates, and accounting for a >3 dB larger implementation penalty for the 16QAM transmitter and receiver pair. Such wide differences between required OSNR and reach between the PM-QPSK and PM-16QAM signals with any given fiber highlight the benefits supplied by flexible transceivers that can change modulation formats and thus data rates. For fiber plant that cannot support 200 Gbits/s data rates with a PM-16QAM signal, the transceiver could reduce the data rate to 100 Gbits/s using PM-QPSK, or perhaps an intermediate format such as PM-8QAM that can be supported over the link length. However, it is worth noting that fibers with ultralow attenuation and larger effective areas will always enable the largest system capacities and longest reach lengths for any given data rate and thus offer the most flexibility to system operators in terms of network configurability.

For Raman systems as studied here, the value of ultralow attenuation also serves to minimize the required Raman pump power. The average total Raman pump powers required by the three different fibers in the PM-16QAM and PM-QPSK systems to fully compensate the span losses are shown in Fig. 8. Note that the pump power required for the SMF-28 ULL fiber systems was about 100 mW lower than that required for the SMF-28e+ fiber systems, because lower total gain was required for the smaller span losses with the ultralow-attenuation fiber. On the other hand, while the Vascade EX2000 fiber has a much larger effective area than the other fibers, and therefore a smaller Raman gain coefficient, the required total pump power was only 85 mW higher than for the SMF-28e+ fiber systems.

One other benefit of ultralow-attenuation, large effective area fiber accrues with the use of Raman amplification, and this is the smaller penalty observed from double Rayleigh backscattering in the fiber [32]. The capture efficiency of the Rayleigh backscattered light is inversely proportional to the fiber effective area, and thus is smaller for larger A_{eff} fibers [33]. This can be observed in Fig. 9, which presents the PM-16QAM signal Q-factor values as a function of OSNR for two fibers investigated here. The data points represent different transmission distances and use the optimal launch powers for each fiber system. The small but measurable advantage of ~0.3–0.4 dBQ of the Vascade EX2000 fiber compared to the standard single-mode fiber

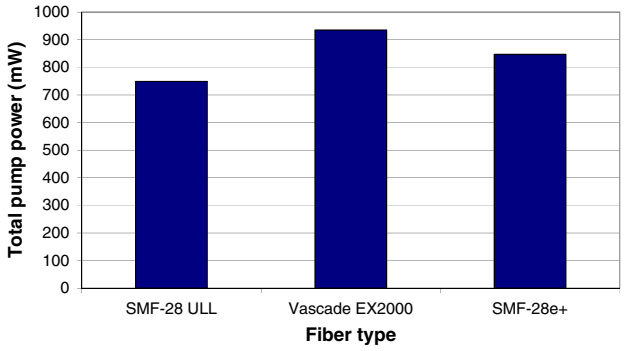

Fig. 8. Raman pump powers required to compensate span losses.

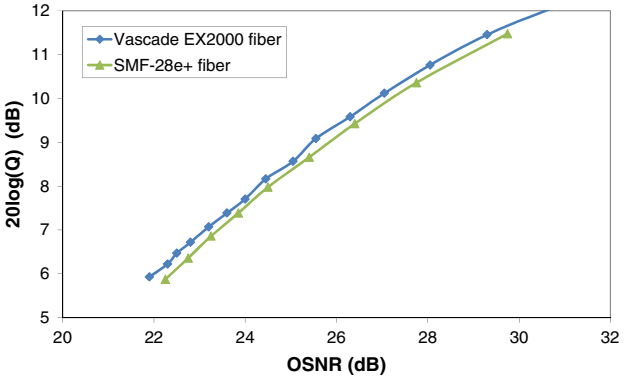

Fig. 9. Q factor versus OSNR for two Raman amplified systems.

illustrates the smaller penalty from double Rayleigh backscatter with that fiber because of its larger effective area and lower attenuation.

As suggested by Figs. 1 and 2, fibers with ultralow attenuation and large effective area offer the best performance in coherent transmission systems. Furthermore, such fibers allow system operators to build networks with lower overall cost by saving on expensive regenerators. Depending on specific conditions, it may also be possible to reduce other costs such as the number of amplifier huts by increasing the system span length. In a recent study, we investigated the application of Vascade EX3000 fiber with nominal 150 μm^2 A_{eff} and ultralow attenuation in transmission systems with average span lengths longer than 100 km [34]. The experimental setup is shown in Fig. 10. Systems with EDFA amplification, 20 channels, and 32 Gbaud symbol rates of either 256 Gbit/s PM-16QAM or 128 Gbit/s PM-QPSK signals were transmitted in a recirculating loop with three spans of length 110, 112, and 115 km. The spans were primarily comprised of 100 km of Vascade EX3000 fiber, with the remainder of each span being Vascade EX2000 fiber.

The optimal channel launch powers were determined to be about the same for the two systems at slightly over 1 dBm/channel. At the optimal power, the two systems were both measured for Q factor and OSNR as functions of distance for the center channel. The results for Q factor and OSNR are shown in Figs. 11 and 12, respectively. As seen with the earlier Raman systems comparison, the reach length of the PM-QPSK system was at least 7× longer

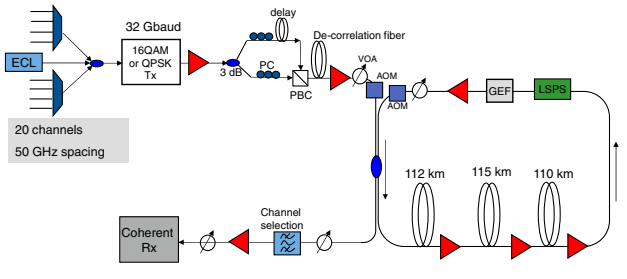

Fig. 10. Experimental setup for transmission performance measurements with long span lengths >100 km.

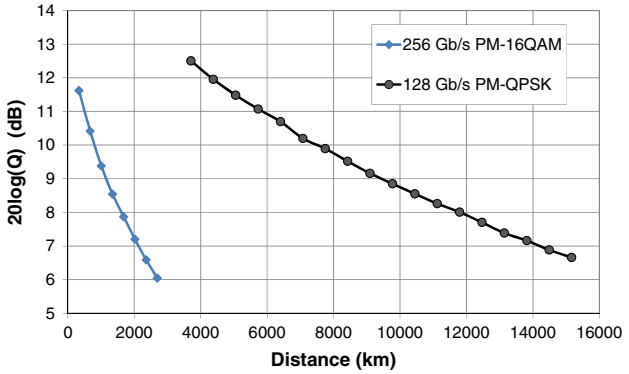

Fig. 11. Q factor as a function of distance for 256 and 128 Gbit/s signals over a system with long span lengths.

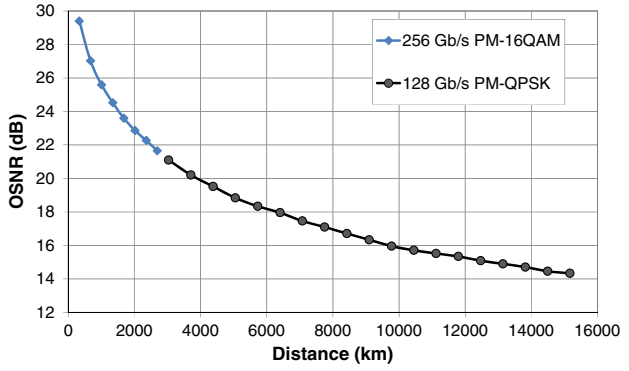

Fig. 12. OSNR as a function of distance for 256 and 128 Gbit/s signals over a system with long span lengths.

than that of the PM-16QAM system as defined at any given Q value. However, the PM-16QAM system had a reach of almost 2400 km at the 6.25 dBQ FEC threshold, and >1000 km with 3 dB margin, sufficient for many terrestrial links. The PM-QPSK system had trans-Atlantic reach of ~8000 km with a more than 3 dBQ margin and OSNR ~17 dB. The ability to use long spans like these with an average length of 112.3 km could reduce the number of repeaters by almost 50% compared to more conventional submarine span lengths of about 60 km.

B. Unrepeatered Submarine Systems

Long point-to-point unrepeatered spans of several hundred kilometers are employed in submarine and terrestrial networks connecting islands to each other and the mainland, mainland points in a festoon configuration, or cities with difficult-to-access terrain between them. In these systems, a key objective is to achieve a single-span system between the points of interest with no active equipment between terminals, and achieving the maximum reach and capacity is critical. There have been many recent research experiments with this type of system for both 100 and 200 Gbit/s channels [35–41].

In terms of optical fiber properties that affect unrepeatered system performance, attenuation and nonlinear tolerance are again central, but their relative importance is changed from the case of repeatered multispan systems. The fiber FOM as defined in Eq. (1) was derived for repeatered systems and may not be strictly applicable to an unrepeatered system, but we can make simple estimations of the different impacts of effective area and attenuation in this context. Specifically, we evaluate the fiber parameters in terms of additional reach, or length of the unrepeatered span, promoted by variations in A_{eff} and attenuation compared to reference values.

Consider first the role of fiber effective area in an unrepeatered span. As for a multispan system, we assume that the channel launch power and nonlinear tolerance are, to first order, directly related to the OSNR of the received signal. Therefore, the difference in OSNR between a fiber with A_{eff} relative to a reference fiber $A_{\text{eff,ref}}$, for the same fiber attenuation, is given by

$$\Delta\text{OSNR(dB)} = 10\ \log\left[\frac{A_{\text{eff}} \cdot n_{2,\text{ref}}}{A_{\text{eff,ref}} \cdot n_2}\right]. \tag{3}$$

The difference in reach for the fiber under evaluation relative to the reference fiber is then simply related to the attenuation of the fibers (assumed equal) as

$$\Delta L = \frac{\Delta\text{OSNR(dB)}}{\alpha_{\text{dB}}}. \tag{4}$$

Using a Ge-doped silica core reference fiber with effective area $A_{\text{eff,ref}} = 80\ \mu\text{m}^2$, results from Eqs. (3) and (4) are shown in Fig. 13 for values of attenuation ranging from 0.15 to 0.18 dB/km. Perhaps the most interesting thing to note is that the absolute difference in reach achievable from larger effective area fibers is relatively small for any attenuation. In fact, the increase in reach ΔL is ≤25 km even for a fiber A_{eff} as large as 170 μm^2. However, the increase is larger for lower attenuation values. Note that the data in Fig. 13 make the same assumption regarding n_2 and attenuation as described earlier. It also does not take

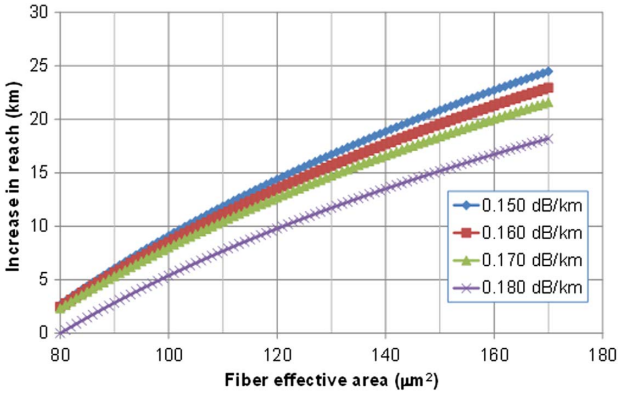

Fig. 13. Increase in unrepeatered span length, or reach, as a function of effective area. Reference fiber effective area = 80 μm^2.

into account any impact of Raman gain on fiber effective area.

Consider next the role of fiber attenuation on the achievable reach of an unrepeatered span system. Such systems can be designed in many different ways, using different configurations of Raman amplification, the use of remote optically pumped amplifiers (ROPAs), etc. However, for a given type of system design, it is common to provide a measure of performance as the total maximum span loss allowed. Using total loss as a metric, we can write that

$$\text{Loss}_{\max}(\text{dB}) = \alpha_{\text{dB}} \cdot L = \alpha_{\text{ref,dB}} \cdot L_{\text{ref}}, \tag{5}$$

where L is the span length for the fiber under evaluation with attenuation α_{dB} and L_{ref} is the span length for the reference fiber. It is then easy to show that the difference in span length or reach, ΔL, between the fiber under evaluation and the reference fiber to the first order is given by

$$\Delta L = \frac{(\alpha_{\text{ref,dB}} - \alpha_{\text{dB}})}{\alpha_{\text{ref,dB}}\alpha_{\text{dB}}} \cdot \text{Loss}_{\max}(\text{dB}). \tag{6}$$

Figure 14 shows ΔL as a function of fiber attenuation for span loss values ranging from 50 to 100 dB. From these results, it is clear that fiber attenuation can have a very significant effect on unrepeatered span length, and has a larger impact than fiber effective area. For example, reducing attenuation from 0.2 to 0.15 dB/km can effectively increase the span length by approximately 80–160 km, depending on allowable span loss.

While a larger fiber effective area allows a higher channel launch power and thus an increase in unrepeatered span reach, Raman gain varies inversely with effective area. Since almost all long unrepeatered span systems rely on Raman gain to help compensate for some of the span loss, hybrid fiber span constructions are often employed to maximize both launch power and Raman gain as well as overall system performance [35,41,42]. In such designs, the larger effective area fiber may be placed at the beginning of the span, where the channel power is highest, and a fiber with a somewhat smaller effective area is placed at the back end of the span to increase Raman gain if backward pumped Raman amplification is used.

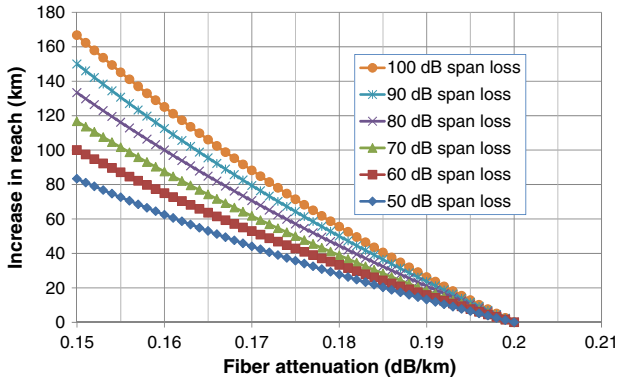

Fig. 14. Increase in unrepeatered span length, or reach, as a function of fiber attenuation. Reference fiber attenuation = 0.20 dB/km.

An example of a recent experiment demonstrating the benefit of hybrid span construction for 256 Gbit/s PM-16QAM transmission over an unrepeatered span utilized ultralow-attenuation fibers with 150 and 112 μm^2 effective areas [41]. The experimental setup is shown in Fig. 15. Forty channels were generated and launched into three different unrepeatered spans for comparison of performance. The first span studied was a 286 km homogeneous fiber span of Vascade EX3000 fiber. The other two span constructions studied were hybrid fiber spans: a 292 km span comprised of 242 km of Vascade EX3000 followed by 50 km of Vascade EX2000 fiber, and a 304 km span comprised of 242 km of Vascade EX3000 plus 62 km of Vascade EX2000 fiber. At the end of each span, amplification of the signals was accomplished by a backward pumped Raman amplifier and an EDFA before detection in the digital coherent receiver. The Raman pump wavelengths were 1427, 1443, and 1461 nm. The pumps had polarization diversity, and the maximum total pump power available was a little over 1 W.

We first measured and compared the Raman ON/OFF gain achieved from the backward pumping in the three span configurations. The Raman gain data at the 1554.13 nm wavelength is shown in Fig. 16 as a function of normalized pump currents used to drive the Raman pump lasers. The data in Fig. 16 clearly show the higher Raman gain achieved in the hybrid spans compared to the homogeneous span, approximately 21 and 14 dB, respectively. This is due to the smaller effective area of the Vascade EX2000 fiber compared to Vascade EX3000 fiber. The higher Raman gain available from the hybrid fiber span designs directly translates into a lower effective noise figure for the Raman/EDFA amplifier combination. This is shown in Fig. 17, where the effective noise figure at 1554.13 nm was calculated from measured OSNR values. At the maximum possible Raman gain, the two hybrid spans have lower effective noise figures than the homogeneous span by about 1.4–1.8 dB.

The Q values of all 40 channels transmitted over the three span configurations are shown together in Fig. 18.

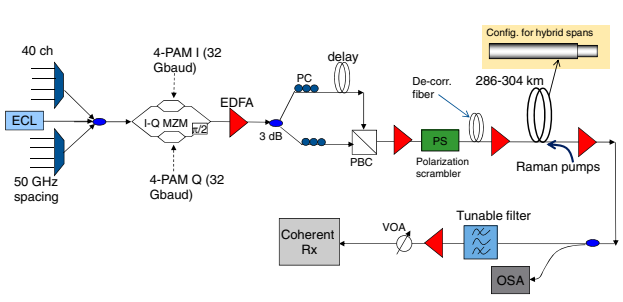

Fig. 15. Experimental setup for unrepeatered span transmission with 256 Gbit/s PM-16QAM signals over homogeneous and hybrid fiber spans. MZM, Mach–Zehnder modulator; PAM, pulse amplitude modulation; PS, polarization scrambler; OSA, optical spectrum analyzer.

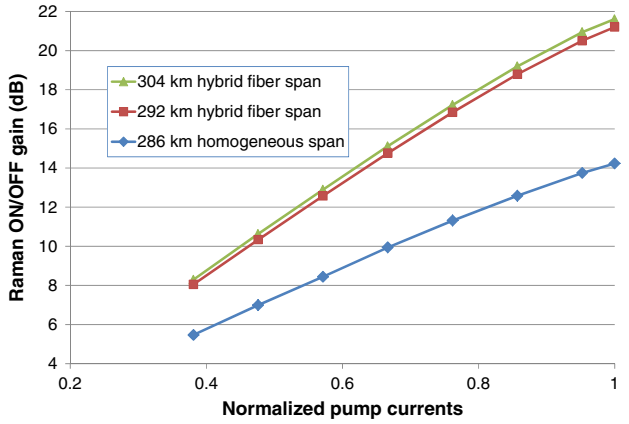

Fig. 16. Measured Raman ON/OFF gain for three unrepeatered spans.

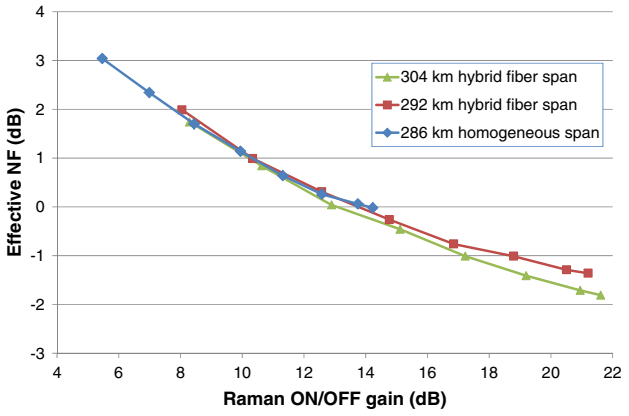

Fig. 17. Effective noise figure (NF) of Raman/EDFA combination for three span configurations.

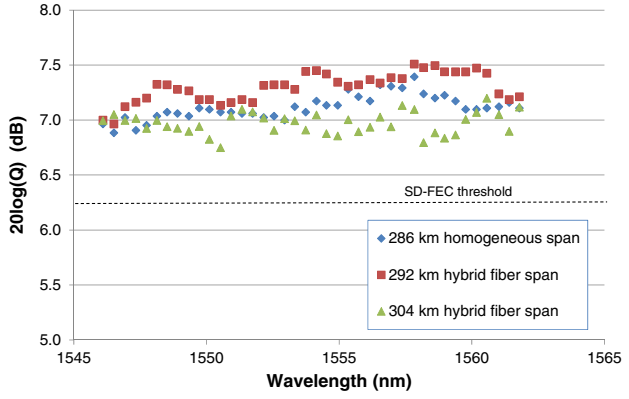

Fig. 18. Q values derived from direct error counting for three unrepeatered span configurations.

Note that the average Q value for the 292 km hybrid span is about 0.2 dB higher than for the 286 km span even though the total span loss is about 1 dB higher. This is because of the lower effective noise figure obtained with higher Raman gain. The 304 km hybrid span system had a total span loss of 47.3 dB. The average Q value for this system was almost 7.0 dB, although we note that for this system the average Q was increased by 0.45 dB by the application of nonlinear compensation applied in the receiver DSP [43,44]. All channels for each of the systems had Q values well above the assumed FEC threshold of 6.25 dB.

Ultimately, to achieve superior transmission performance in unrepeatered systems, both advanced fibers and advanced equipment must be used. Hero transmission experiments also frequently use ROPAs, pumped either through a fiber used for data transmission or a dedicated fiber. As a result of innovations in fibers and active equipment, the maximum unrepeatered distances at 100 Gbits/s increased from 500 to 610 km [45–48] only over the course of 18 months. Most recently, 100 Gbits/s unrepeatered transmission with a span loss of over 100 dB was achieved, corresponding to a record 626.8 km of transmission distance [49].

C. Practical Considerations When Splicing Large Effective Area Fibers

Large effective area fibers are sometimes perceived to suffer from higher splice loss compared to G.652 fibers. This is generally true when a large A_{eff} fiber is spliced to a G.652 fiber, and the splice loss depends on the magnitude of difference in A_{eff} values. The necessity for splicing fibers with dissimilar A_{eff} values may occur when a large A_{eff} transmission fiber is connected to a G.652 fiber in an EDFA pigtail at the two ends of the transmission span. However, even though two such splices are made, only the losses arising from the second splice (i.e., at the very end of the span) matter from a transmission performance standpoint. This is because the loss of the first splice can be compensated by increasing power at the output of the EDFA, without an increase in nonlinear effects within the transmission fiber.

However, it must also be noted that within the transmission span multiple splices between large A_{eff} fibers will be made. In terrestrial networks the number of splices per amplifier span is typically higher than in submarine networks, and is determined by the cable drum, usually in the range of 2–8 km. Our measurements showed that the typical splice loss between two large A_{eff} fibers is lower than the splice loss between two G.652 fibers. This is because for the same amount of radial offset during the splice, the relative mode field diameter mismatch for two large A_{eff} fibers is smaller than for two G.652 fibers. The average splice losses between different fibers are summarized in Table II; the results were obtained by performing multiple splices involving low, medium, and high A_{eff} of a particular fiber type and averaging out the data [26].

If we investigate a hypothetical scenario with 80 km spaced amplifiers and splices performed every 5 km, it becomes apparent that the use of Vascade EX2000 fiber provides lower overall splice loss than G.652 fiber (Table III).

TABLE II
AVERAGE SPLICE LOSS (DB)

Vascade EX3000 Fiber–Vascade EX3000 Fiber	Vascade EX2000 Fiber–Vascade EX2000 Fiber	G.652 Fiber–G.652 Fiber	Vascade EX2000 Fiber–G.652 Fiber	Vascade EX3000 Fiber–G.652 Fiber	Vascade EX3000 Fiber–G.652 Fiber (w. Bridge Fiber)
0.014	0.017	0.024	0.065	0.296	0.162

TABLE III
SPLICE LOSSES FOR AN 80 KM SPAN WITH SPLICES EVERY 5 KM (DB)

	Total Similar A_{eff} Splice Loss Within Span	Splice Loss at EDFA	Total Splice Loss
G.652 fiber	0.36	0.024	0.384
Vascade EX2000 fiber	0.255	0.065	0.32
Vascade EX3000 fiber	0.21	0.296	0.506
Vascade EX3000 fiber (w. bridge fiber)	0.21	0.162	0.372

The use of Vascade EX3000 fiber, on the other hand, leads to a modest 0.122 dB increase in total splice loss compared to G.652 fiber. However, this additional loss is much lower than the reduction in loss due to the difference in attenuation between Vascade EX3000 fiber and G.652 fiber. Furthermore, to offset the small increase in splice loss, a practice involving a "bridge" fiber is frequently used. In this work we used Vascade EX2000 fiber with an intermediate A_{eff} as a "bridge" fiber to show that this approach yields the same or lower total splice loss compared to a G.652-only ecosystem [26]. Table III shows that while the use of "bridge" fiber requires two splices to be performed, the overall average span splice loss for Vascade EX3000 fiber can be reduced below that for G.652 fiber.

III. CONCLUSION

We have examined the characteristics of optical fibers that are most critical to system-level performance in modern optical networks. With coherent transmitter/receivers operating at high data rates of 100 Gbits/s and above, the attributes of fiber attenuation and nonlinear tolerance, mainly via fiber effective area, have the most impact on system reach and flexibility that may help promote network elasticity. While both lower attenuation and larger effective area can comparably increase reach and performance for multispan repeatered systems, the role of attenuation assumes disproportionate importance for long single-span unrepeatered systems. We have illustrated the performance advantages of ultralow attenuation large effective area fibers for 100 and 200 Gbit/s transmission for several different amplification and system configurations.

REFERENCES

[1] F. P. Kapron, D. B. Keck, and R. D. Maurer, "Radiation losses in glass optical waveguides," *Appl. Phys. Lett.*, vol. 17, pp. 423–425, 1970.

[2] D. J. Richardson, J. M. Fini, and L. E. Nelson, "Space-division multiplexing in optical fibres," *Nat. Photonics*, vol. 7, pp. 354–362, 2013.

[3] R. J. Sanferrare, "Terrestrial lightwave systems," *AT&T Tech. J.*, vol. 66, no. 1, pp. 95–107, 1987.

[4] W. B. Joyce, R. W. Dixon, and R. L. Hartman, "Statistical characterization of the lifetimes of continuously operated (Al, Ga)As double-heterostructure lasers," *Appl. Phys. Lett.*, vol. 28, no. 11, pp. 684–686, 1976.

[5] B. J. Ainslie, K. J. Beales, C. R. Day, and J. D. Rush, "The design and fabrication of monomode optical fiber," *IEEE J. Quantum Electron.*, vol. 18, pp. 514–523, 1982.

[6] P. D. Lazay and A. D. Pearson, "Developments in single mode fibre design, materials, and performance at Bell Laboratories," *IEEE J. Quantum Electron.*, vol. 18, pp. 504–510, 1982.

[7] C. A. Miller, M. H. Reeve, S. Hornung, and D. B. Payne, "Optimum design of 1.3- and 1.55-μm monomode fiber," in *Optical Fiber Communication Conf. (OFC)*, 1983, paper MF2.

[8] L. G. Cohen, C. Lin, and W. G. French, "Tailoring zero chromatic dispersion into the 1.5–1.6 pm low-loss spectral region of single-mode fibres," *Electron. Lett.*, vol. 15, pp. 334–335, 1979.

[9] W. A. Gambling, H. Matsumura, and C. M. Ragdale, "Zero total dispersion in graded-index single mode fibres," *Electron. Lett.*, vol. 15, pp. 474–476, 1979.

[10] V. A. Bhagavatula, M. S. Spotz, and D. E. Quinn, "Uniform waveguide dispersion segmented-core designs for dispersion-shifted single-mode fibers," in *Optical Fiber Communication Conf. (OFC)*, 1984, paper. MG2.

[11] D. M. Cooper, S. P. Craig, B. J. Ainslie, and C. R. Day, "Dispersion shifted single-mode fibers using multiple index structures," *Brit. Telecommun. Technol. J.*, vol. 3, pp. 52–58, 1985.

[12] R. W. Tkach, A. R. Chraplyvy, F. Forghieri, A. H. Gnauck, and R. M. Derosier, "Four-photon mixing and high-speed WDM systems," *J. Lightwave Technol.*, vol. 13, no. 5, pp. 841–849, 1995.

[13] G. P. Agrawal, *Nonlinear Fiber Optics*. San Diego, CA: Academic, 1989.

[14] M. A. Newhouse, L. J. Button, D. Q. Chowdhury, Y. Liu, and V. L. Da Silva, "Optical amplifiers and fibers for multiwavelength systems," in *Annu. Meeting Lasers and Electro-Optics Society*, 1995, pp. 44–45.

[15] P. Nouchi, P. Sansonetti, S. Landais, G. Barre, C. Brehm, J. Y. Noniort, B. Perrin, J. J. Girard, and J. Auge, "Low-loss single-mode fiber with high nonlinear effective area," in *Optical Fiber Communication Conf. (OFC)*, 1995, pp. 260–261.

[16] V. L. Da Silva, Y. Liu, D. Q. Chowdhury, M.-J. Li, A. J. Antos, and A. F. Evans, "Error free WDM transmission of 8 × 10 Gbit/s over km of LEAF optical fiber," in *Proc. European Conf. on Optical Communication*, 1997, pp. 154–158.

[17] D. W. Peckham, A. F. Judy, and R. B. Kummer, "Reduced dispersion slope, non-zero dispersion fiber," in *Proc. European Conf. on Optical Communication*, 1998, pp. 139–140.

[18] Y. Liu, "Dispersion shifted large-effective-area fiber for amplified high-capacity long-distance systems," in *Optical Fiber Communication Conf. (OFC)*, 1997, pp. 16–21.

[19] P. Nouchi, "Maximum effective area for non-zero dispersion-shifted fiber," in *Optical Fiber Communication Conf. (OFC)*, 1998, pp. 303–304.

[20] P. Nouchi, P. Sansonetti, J. Von Wirth, and C. Le Sergent, "New dispersion shifted fiber with effective area larger than 90 μm^2," in *Proc. European Conf. on Optical Communication*, 1996, pp. 49–52.

[21] Y. Liu and G. Berkey, "Single-mode dispersion-shifted fibers with effective area over 100 μm^2," in *Proc. European Conf. on Optical Communication*, 1998, pp. 41–42.

[22] J. Kahn and K.-P. Ho, "Spectral efficiency limits and modulation/detection techniques for DWDM systems," *IEEE J. Sel. Top. Quantum Electron.*, vol. 10, pp. 259–272, 2004.

[23] K. Roberts, M. O'Sullivan, K.-T. Wu, H. Sun, A. Awadalla, D. J. Krause, and C. Laperle, "Performance of dual-polarization QPSK for optical transport systems," *J. Lightwave Technol.*, vol. 27, pp. 3546–3559, Aug. 2009.

[24] A. Bononi, P. Serena, N. Rossi, and D. Sperti, "Which is the dominant nonlinearity in long-haul PDM-QPSK coherent transmissions?" in *Proc. European Conf. on Optical Communication*, 2010, paper Th.10.E.1.

[25] V. Curri, A. Carena, G. Bosco, P. Poggiolini, M. Hirano, Y. Yamamoto, and F. Forghieri, "Fiber figure of merit based on maximum reach," in *Optical Fiber Communication Conf. (OFC)*, 2013, paper OTh3G.2.

[26] S. Makovejs, J. D. Downie, J. E. Hurley, J. S. Clark, I. Roudas, C. C. Roberts, H. B. Matthews, F. Palacios, D. A. Lewis, D. T. Smith, P. G. Diehl, J. J. Johnson, C. R. Towery, and S. Y. Ten, "Towards superior transmission performance in submarine systems: Leveraging ultra-low attenuation and large effective area," *J. Lightwave Technol.*, vol. 34, pp. 114–120, 2016.

[27] K. S. Kim, R. H. Stolen, W. A. Reed, and K. W. Quoi, "Measurement of the nonlinear index of silica-core and dispersion-shifted fibers," *Opt. Lett.*, vol. 19, pp. 257–259, 1994.

[28] W. A. Wood, S. Ten, I. Roudas, P. M. Sterlingov, N. Kaliteevskiy, J. D. Downie, and M. Rukosueva, "Relative importance of optical fiber effective area and attenuation in span length optimization of ultra-long 100 Gb/s PM-QPSK systems," in *SubOptic*, 2013, paper TU1 C-3.

[29] J. D. Downie, "112 Gb/s PM-QPSK transmission systems with reach lengths enabled by optical fibers with ultra-low loss and very large effective area," *Proc. SPIE*, vol. 8284, 828403, 2012.

[30] J. D. Downie, J. Hurley, D. Pikula, S. Ten, and C. Towery, "Study of EDFA and Raman system transmission reach with 256 Gb/s PM-16QAM signals over three optical fibers with 100 km spans," *Opt. Express*, vol. 21, pp. 17372–17378, 2013.

[31] O. Bertran-Pardo, J. Renaudier, H. Mardoyan, P. Tran, F. Vacondio, M. Salsi, G. Charlet, S. Bigo, A. Konczykowska, J.-I. Dupuy, F. Jorge, M. Riet, and J. Godin, "Experimental assessment of transmission reach for uncompensated 32-GBaud PDM-QPSK and PDM-16QAM," in *Optical Fiber Communication Conf. (OFC)*, 2012, paper JW2A.53.

[32] J. Bromage, P. J. Winzer, and R.-J. Essiambre, "Multiple path interference and its impact on system design," in *Raman Amplifiers for Telecommunications 2*, M. Islam, Ed. New York: Springer-Verlag, 2004, pp. 491–568.

[33] E. Brinkmeyer, "Analysis of the backscattering method for single-mode optical fibers," *J. Opt. Soc. Am.*, vol. 70, pp. 1010–1012, 1980.

[34] J. D. Downie, J. Hurley, and D. Pikula, "Transmission of 256 Gb/s PM-16QAM and 128 Gb/s PM-QPSK signals over long-haul and submarine systems with span lengths greater than 100 km," in *Proc. European Conf. on Optical Communication*, 2013, paper Tu.1.D.3.

[35] J. D. Downie, J. Hurley, J. Cartledge, S. Ten, S. Bickham, S. Mishra, X. Zhu, and A. Kobyakov, "40 × 112 Gb/s transmission over an unrepeatered 365 km effective area-managed span comprised of ultra-low loss optical fibre," in *Proc. European Conf. on Optical Communication*, 2010, paper We.7.C.5.

[36] D. Mongardien, P. Bousselet, O. Bertran-Pardo, P. Tran, and H. Bissessur, "2.6Tb/s (26 × 100 Gb/s) unrepeatered transmission over 401 km using PDM-QPSK with a coherent receiver," in *Proc. European Conf. on Optical Communication*, 2009, paper 6.4.3.

[37] H. Bissessur, P. Bousselet, D. Mongardien, G. Boissy, and J. Lestrade, "4 × 100 Gb/s unrepeatered transmission over 462 km using coherent PDM-QPSK format and real-time processing," in *Proc. European Conf. on Optical Communication*, 2011, paper Tu.3.B.3.

[38] D. Chang, W. Pelouch, and J. McLaughlin, "8 × 120 Gb/s unrepeatered transmission over 444 km (76.6 dB) using distributed Raman amplification and ROPA without discrete amplification," in *Proc. European Conf. on Optical Communication*, 2011, paper Tu.3.B.2.

[39] S. Oda, T. Tanimura, Y. Cao, T. Hoshida, Y. Akiyama, H. Nakashima, C. Ohshima, K. Sone, Y. Aaoki, M. Yan, Z. Tao, J. C. Rasmussen, Y. Yamamoto, and T. Sasaki, "80 × 224 Gb/s unrepeated transmission over 240 km of large-A_{eff} pure silica core fibre without remote optical pre-amplifier," in *Proc. European Conf. on Optical Communication*, 2011, paper Th.13.C.7.

[40] D. Mongardien, C. Bastide, B. Lavigne, S. Etienne, and H. Bissessur, "401 km unrepeatered transmission of dual-carrier 400 Gb/s PDM-16QAM mixed with 100 Gb/s channels," in *Proc. European Conf. on Optical Communication*, 2013, paper Tu.1.D.2.

[41] J. D. Downie, J. Hurley, I. Roudas, D. Pikula, and J. A. Garza-Alanis, "256 Gb/s PM-16QAM unrepeatered transmission over up to 304 km with simple system configurations," *Opt. Express*, vol. 22, pp. 10256–10261, 2014.

[42] A. Puc, D. Chang, W. Pelouch, P. Perrier, D. Krishnappa, and S. Burtsev, "Novel design of very long, high capacity unrepeatered Raman links," in *Proc. European Conf. on Optical Communication*, 2009, paper 6.4.2.

[43] E. Ip and J. M. Kahn, "Compensation of dispersion and nonlinear impairments using digital backpropagation," *J. Lightwave Technol.*, vol. 26, pp. 3416–3425, 2008.

[44] E. Ip, "Nonlinear compensation using backpropagation for polarization-multiplexed transmission," *J. Lightwave Technol.*, vol. 28, pp. 939–951, 2010.

[45] V. Gainov, N. Gurkin, S. Lukinih, S. Makovejs, S. Akopov, S. Ten, O. Nanii, V. Treshchikov, and M. Sleptsov, "Record 500 km unrepeatered 1 Tbit/s (10 × 100 G) transmission over an ultra-low loss fiber," *Opt. Express*, vol. 22, no. 19, pp. 22308–22313, 2014.

[46] T. J. Xia, D. L. Peterson, G. A. Wellbrock, D. Chang, P. Perrier, H. Fevrier, S. Ten, C. Towery, and G. Mills, "557-km unrepeatered 100 G transmission with commercial Raman WDM system, enhanced ROPA, and cabled large A_{eff} ultra-low loss

fiber in OSP environment," in *Optical Fiber Communication Conf. (OFC)*, 2014, paper Th5A.7.

[47] D. Chang, P. Perrier, H. Fevrier, S. Makovejs, C. Towery, X. Jia, L. Deng, and B. Li, "Ultra-long unrepeatered transmission over 607 km at 100 G and 632 km at 10 G," *Opt. Express*, vol. 23, no. 19, pp. 25028–25033, 2015.

[48] S. Etienne, H. Bissessur, C. Bastide, and D. Mongardien, "Ultra-long 610 km unrepeatered transmission of 100 Gb/s using single fibre configuration," in *Proc. European Conf. on Optical Communication*, 2015, paper Th.2.2.5.

[49] D. Chang, E. Zak, W. Pelouch, P. Perrier, H. Fevrier, L. Deng, B. Li, S. Makovejs, C. Hao, J. Xu, and M. Xiang, "100 G unrepeatered transmission over 626.8 km with a span loss in excess of 100 dB," in *Proc. Asia Communications Photonics Conf.*, 2015, paper AM4A.2.

John D. Downie received a B.S. degree in optics from the University of Rochester, Rochester, NY, in 1983, a Certificate of Postgraduate Study in physics from Cambridge University, Cambridge, UK, in 1984, and his M.S. and Ph.D. degrees in electrical engineering from Stanford University, Stanford, CA, in 1985 and 1989, respectively. He has been a member of IEEE since 2008. In 1989, he joined the National Aeronautics and Space Administration (NASA) Ames Research Center, where he was a Research Scientist and Group Leader of the Information Physics Research Group, conducting research in optical information processing and optical data storage. He joined Corning Incorporated, Corning, NY, in 1999 as a Research Associate in the Science and Technology Division. He became a Senior Research Associate in 2007. He has authored or co-authored more than 140 journal and conference papers to date. His current research interests at Corning are mainly focused on optical fibers and transmission systems for all length scales. Dr. Downie has been a member of The Optical Society (OSA) since 1984, including senior membership since 2007. He was awarded the Churchill Foundation Scholarship to study at Cambridge University in 1983. Dr. Downie regularly serves as a reviewer for IEEE and OSA optics journals.

Ming-Jun Li received a B.Sc. degree in applied physics from the Beijing Institute of Technology, Beijing, China, in 1983, an M.Sc. degree in optics and signal processing from University of Franche-Comté, Besancon, France, in 1985, and a Ph.D. degree in physics from University of Nice, Nice, France, in 1988. He joined Corning Incorporated in 1991 and is currently a Corporate Fellow. He has been a key inventor and contributor to many telecom and specialty fibers including bend-insensitive ClearCurve optical fiber for fiber to the home, which received the R&D 100 Award and was featured as one of *Time* magazine's "Best Inventions of the Year"; LEAF fiber, which won four industrial awards and was deployed with more than 30 million kilometers of fiber in long-haul networks; ultralow PMD fiber and low-loss fiber for high-data-rate transmission; low stimulated Brillouin scattering fiber for analog signal transmission; high-bandwidth multimode fiber for data centers; various specialty fibers for use in connectors, fiber lasers, sensors and endoscopes; and new multicore fibers and few-mode fibers for future space-division multiplexing. Recently, he also has been working on new glass measurement techniques for measuring chemically strengthened glass and laminate glass and creating optical functionalities on glass substrates. His research efforts have resulted in the generation of a significant number of new products and revenue. Dr. Li received the 1988 French National Prize on Guidedwave Optics for his work on Cerenkov second-harmonic generation, the 2005 Stookey Award for exploratory research at Corning Incorporated, and the 2008 Northeast Regional Industrial Innovation Award from the American Chemical Society. He is a Fellow of IEEE and OSA. He has served as Associate Editor and Coordinating Committee Member and currently is Deputy Editor for the *Journal of Lightwave Technology*. He also has served as a guest editor for several special journal issues and as committee chair or member for many international conferences. Dr. Li holds 131 U.S. patents and has published three book chapters and authored or co-authored over 230 technical papers in journals and conferences.

Sergejs Makovejs obtained his B.Sc. and M.Sc. degrees in telecommunications from Riga Technical University, Latvia, in 2004 and 2006, respectively, and his Ph.D. degree in electronic and electrical engineering from University College London, UK, in 2011. He presently works at Corning Limited, UK, on the Market and Technology Development Team of the Optical Communications Division; from 2011 to April 2015 he worked at Corning Incorporated, USA. He has authored or co-authored more than 20 peer-reviewed journal and conference papers in the field of optical fiber communication systems. From 2006 to 2007, he also worked at Siemens, where he was involved in designing rail automation and signaling systems. His current professional interests include metro, long-haul terrestrial, and submarine networks. Dr. Makovejs has previously served as a reviewer for *IEEE Photonics Technology Letters* and *Optics Express*. In 2010 he was shortlisted in the Outstanding Student Paper Competition at the Optical Fiber Communication Conference and was awarded a Royal Academy of Engineering travel grant to present his work. Dr. Makovejs is a regular presenter at technical conferences and seminars.